Ruthenium Anchored Zirconium Dioxide Derived from Metal-Organic Framework as a Highly Efficient pH-Universal Electrocatalyst for Hydrogen Evolution

Liyun Cao,[a] Wenchao Li,[a] Jianfeng Huang,*[a] Dewei Chu,[b] Yijun Liu,[c] Faliang Luo,[d] Xuemeng Huo,[a] Dongping Wang,[a] Yongqiang Feng*[a]*

[a]School of Material Science and Engineering, International S&T Cooperation Foundation of Shaanxi Province, Shaanxi University of Science and Technology, Xi'an, 710021, China

[b]School of Materials Science and Engineering, University of New South Wales, Sydney, NSW 2052, Australia

[c]Mona Lisa Group Co. Ltd., Foshan, Guangdong 528211, PR China

[d]State Key Laboratory of High-efficiency Coal Utilization and Green Chemical Engineering, College of Chemistry and Chemical Engineering, Ningxia University, Yinchuan, 750021, China

E-mail: caoliyun@sust.edu.cn; huangjf@sust.edu.cn; fengyq@sust.edu.cn

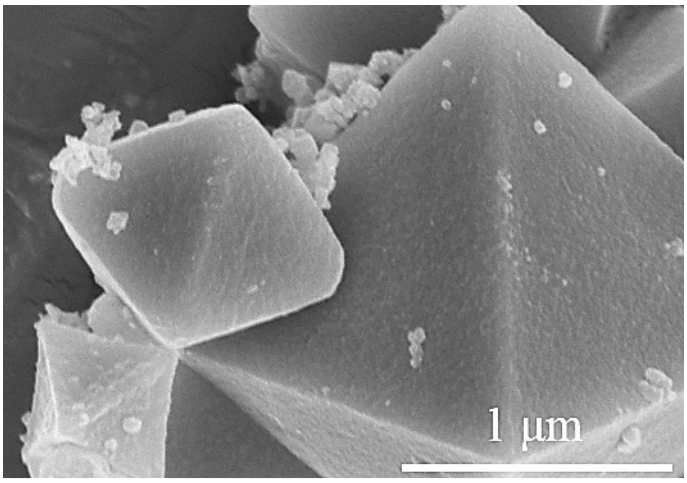

Fig. S1. SEM images of UiO-bpy.

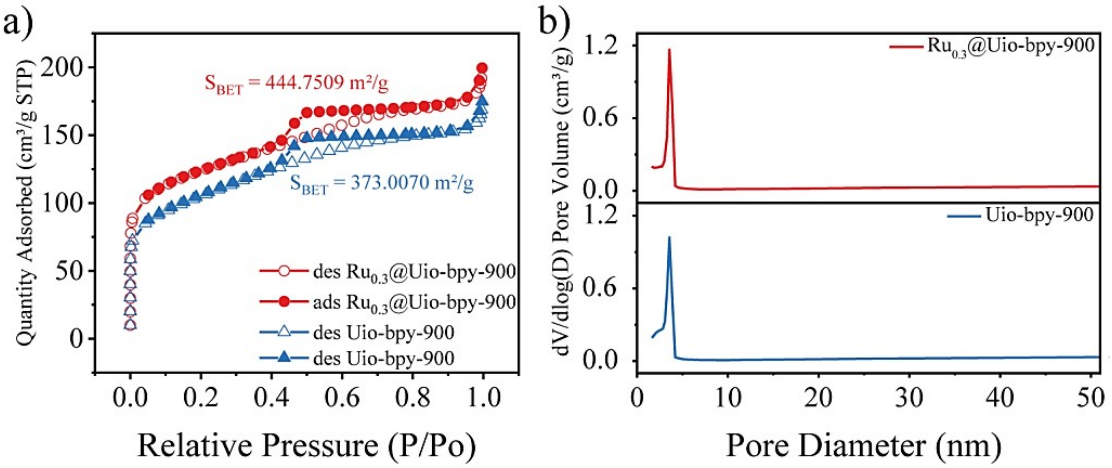

Fig. S2. (a) Nitrogen gas adsorption (solid) and desorption (empty) isothermal curves, (b) Corresponding pore size distribution curves of $Ru_{0.3}$@UiO-bpy-900 and UiO-bpy-900.

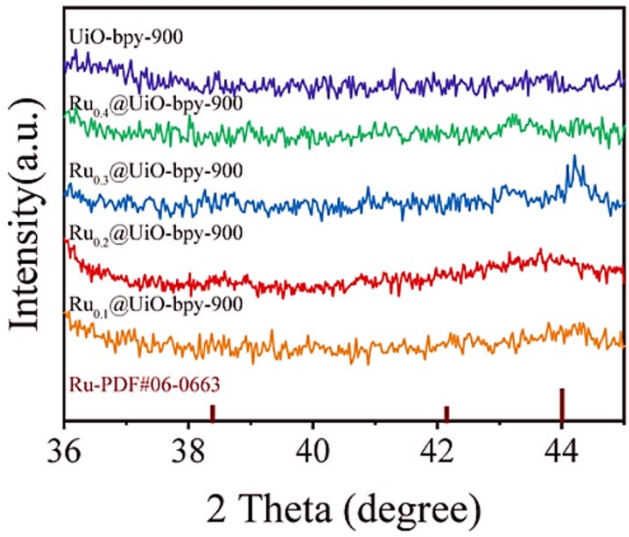

Fig. S3. XRD pattern of Ru_x@UiO-bpy-900 (x = 0.1，0.2，0.3 and 0.4 mmol) in the diffraction angles from 36 to 45.

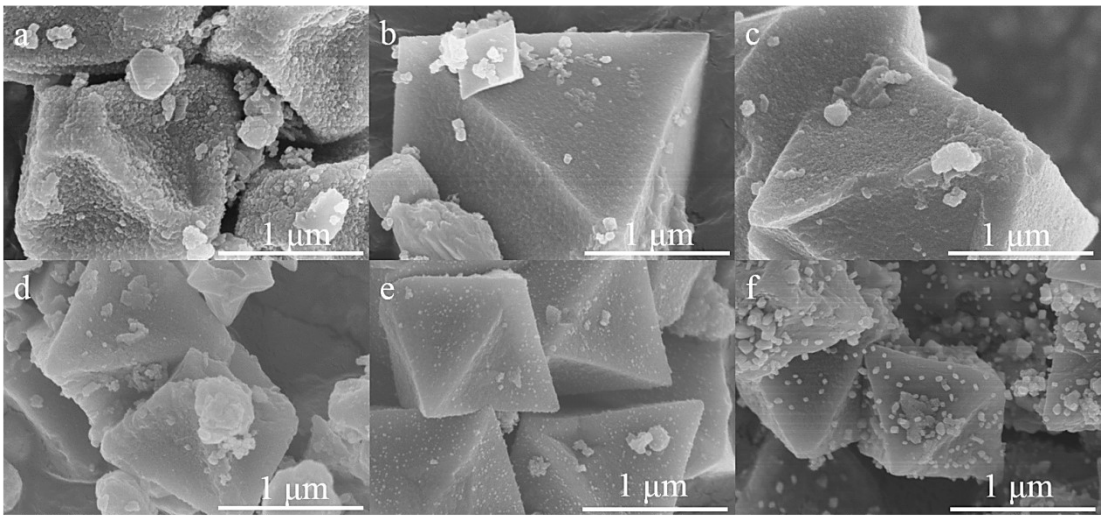

Fig. S4. SEM image of (a-c) Ru_x@UiO-bpy (x=0.1, 0.2, 0.4) and (d-f) Ru_x@UiO-bpy-900(x=0.1, 0.2, 0.4)

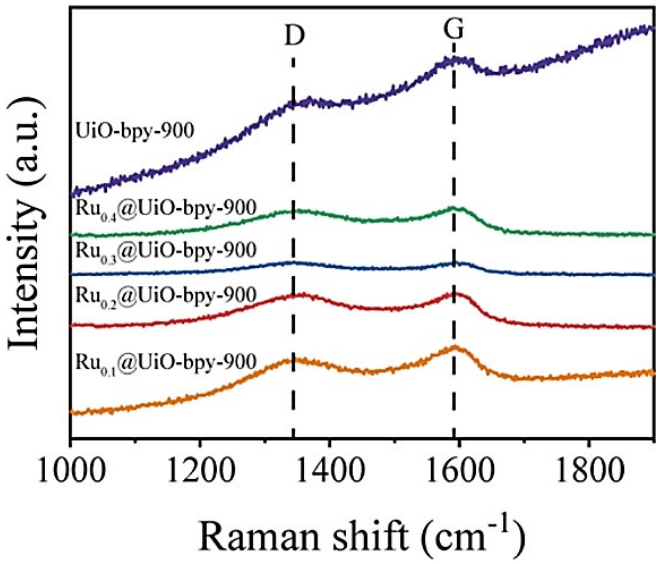

Fig. S5. Raman spectrum of Ru_x@UiO-bpy-900 and UiO-bpy-900

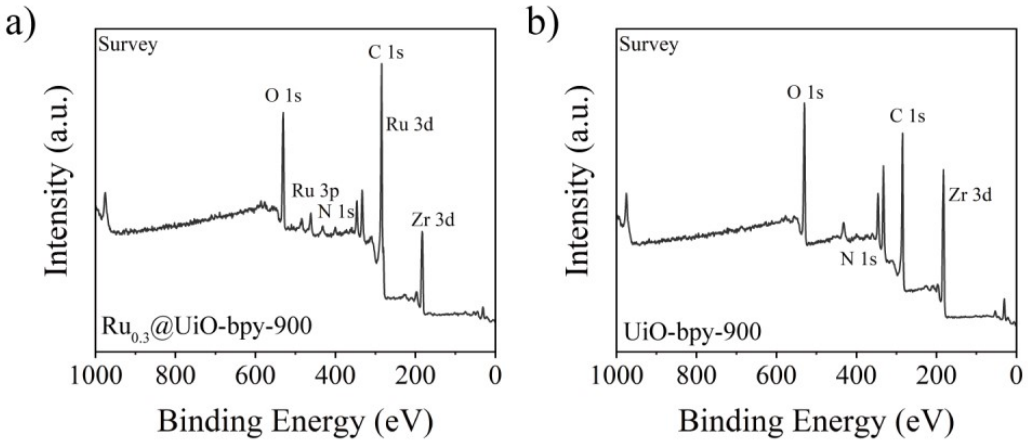

Fig. S6. XPS survey spectra of (a) $Ru_{0.3}$@UiO-bpy-900 and (b) UiO-bpy-900

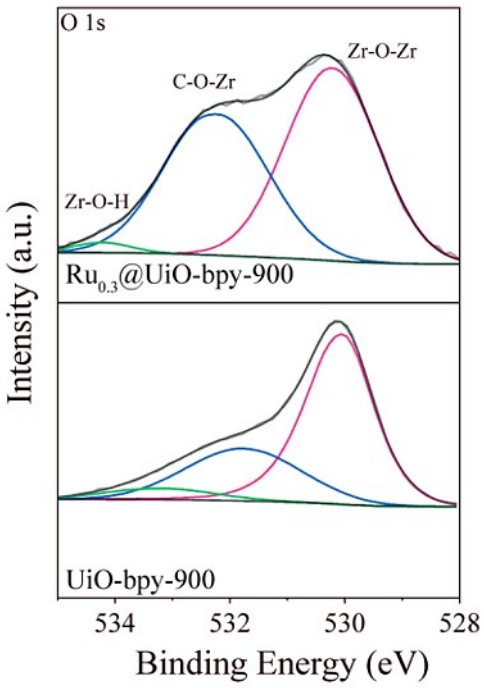

Fig. S7. O 1s of $Ru_{0.3}$@UiO-bpy-900 and UiO-bpy-900.

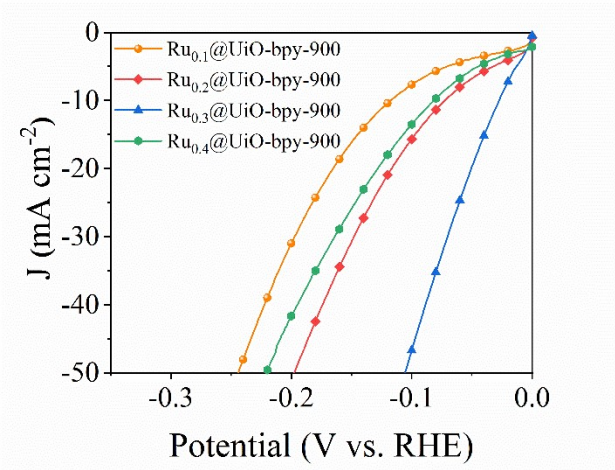

Fig. S8. LSV curve of Ru_x@UiO-bpy-900 (x = 0.1,0.2 ,0.3 and 0.4 mmol) in 1 M KOH

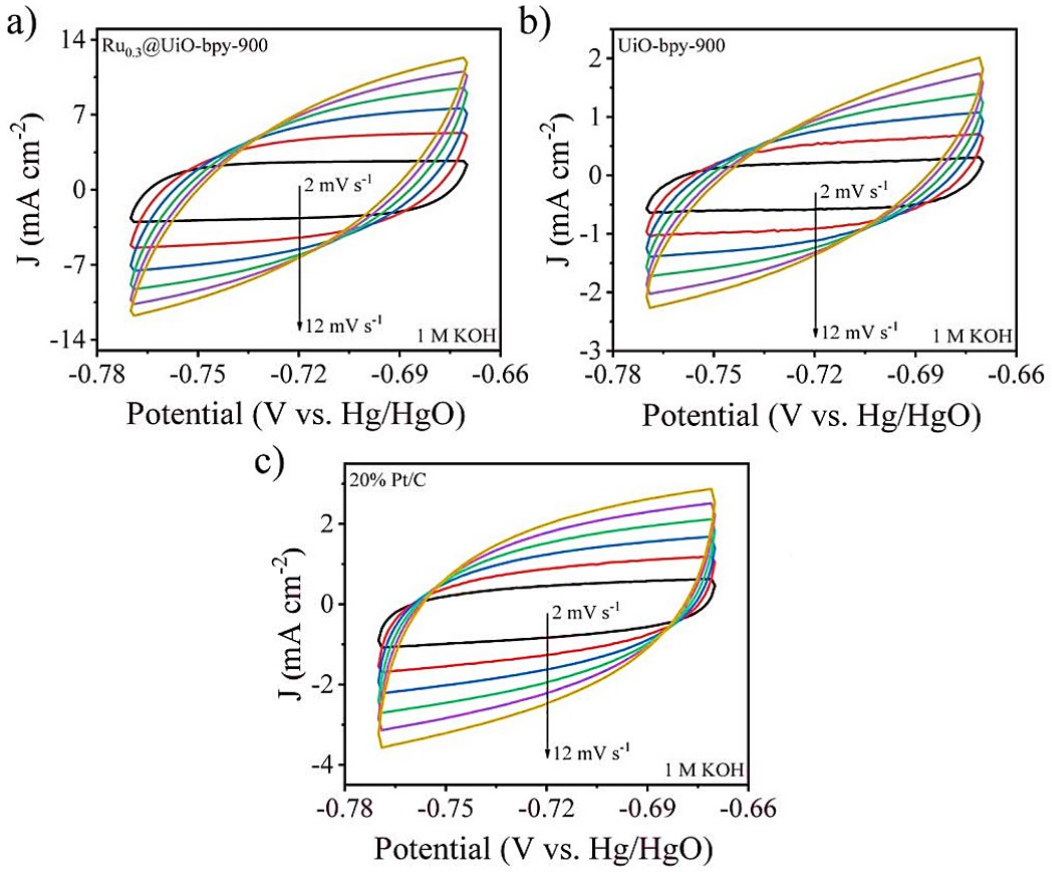

Fig. S9. CV curves with scan rates of 2, 4, 6, 8, 10 and 12 mV s^{-1} of a) $Ru_{0.3}$@UiO-bpy-900, b) UiO-bpy-900, c) 20% Pt/C in 1 M KOH

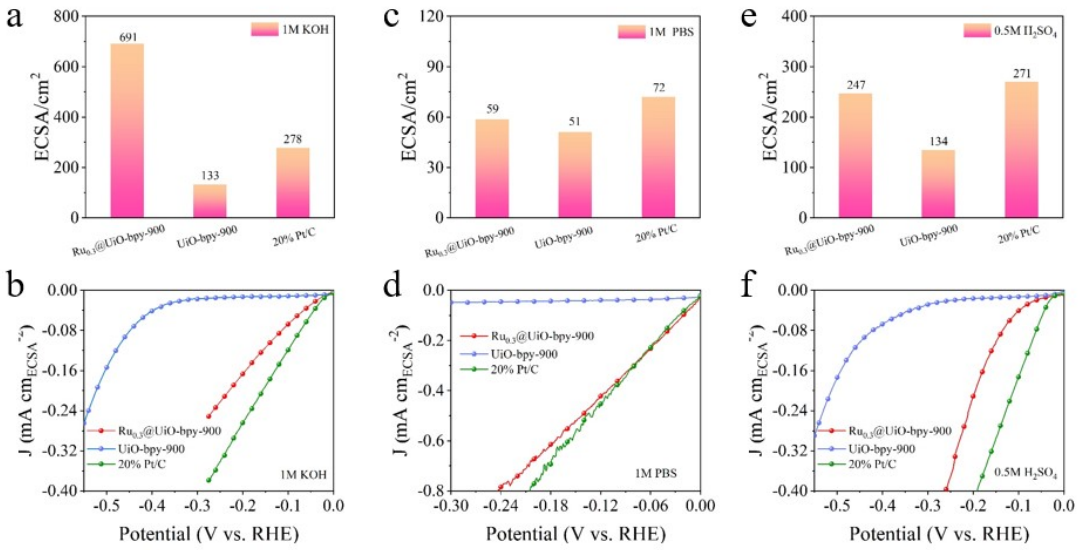

Fig. S10. The electrochemical active specific surface area and the ECSA-normalized LSV of $Ru_{0.3}$@UiO-bpy-900, UiO-bpy-900 and commercial benchmark 20% Pt/C in different electrolytes. (a, b) 1 M KOH, (c, d) 1 M PBS, (e, f) 0.5 M H_2SO_4.

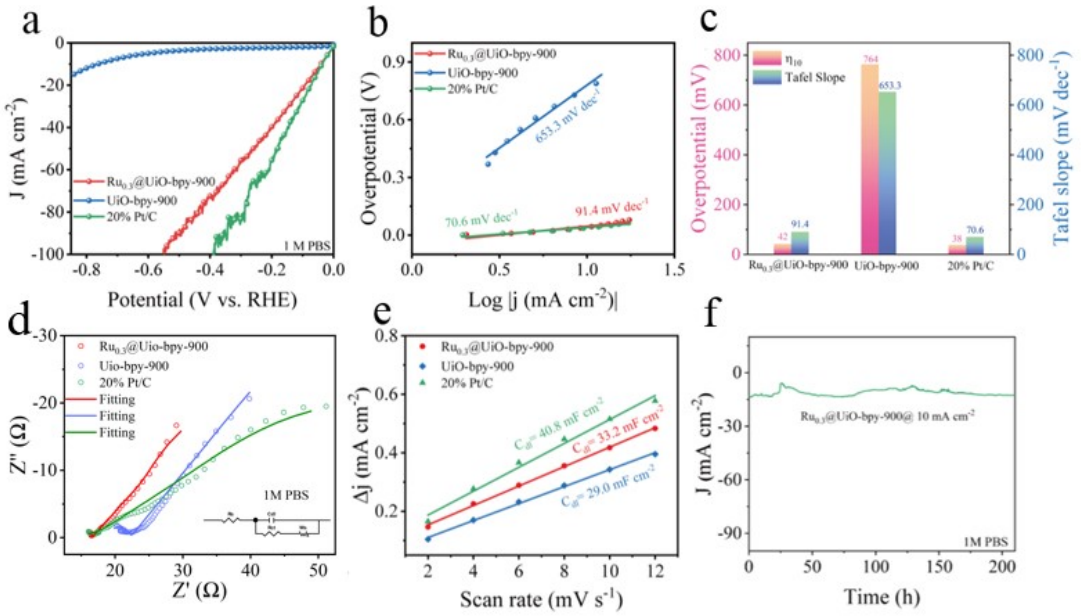

Fig. S11. Electrochemical HER performance in 1.0 M PBS. (a) The LSV curves, (b) Tafel plots, (c) the histograms of overpotential and Tafel slopes, (d) Nyquist plot and the fitting curves, (e) current density difference against scan rate of $Ru_{0.3}$@UiO-bpy-900, UiO-bpy-900 and the commercial benchmark 20% Pt/C. (f) Long-term chronoamperometric test of $Ru_{0.3}$@UiO-bpy-900.

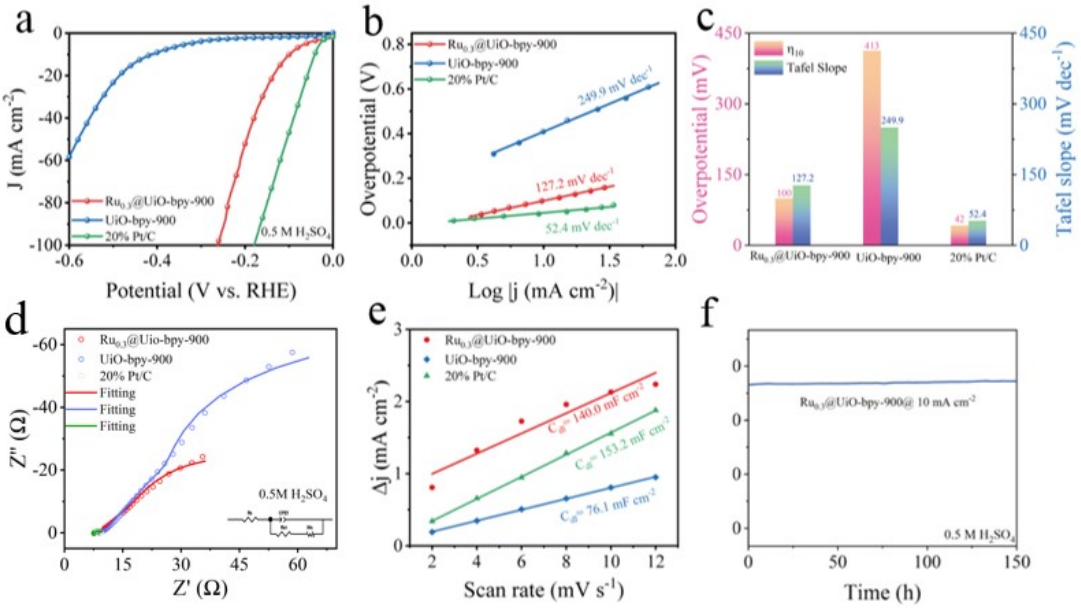

Fig. S12. Electrochemical HER performance in 0.5 M H_2SO_4. (a) The LSV curves, (b) Tafel plots, (c) the histograms of overpotential and Tafel slopes, (d) Nyquist plot and the fitting curves, (e) current density difference against scan rate of $Ru_{0.3}$@UiO-bpy-900, UiO-bpy-900 and the commercial benchmark 20% Pt/C. (f) Long-term chronoamperometric test of $Ru_{0.3}$@UiO-bpy-900.

Table S1 EIS fitting parameters for $Ru_{0.3}$@UiO-bpy-900, UiO-bpy-900, and Commercial 20% Pt/C in 1.0 M KOH

Sample	Element	Value	Error %
$Ru_{0.3}$@UiO-bpy-900	Rs	1.437	4.964
	Rct	15.32	1.5286
UiO-bpy-900	Rs	1.241	7.0699
	Rct	24	0.56654
20% Pt/C	Rs	1.502	5.282
	Rct	15.89	1.1658